

One-pot hydrothermal synthesise and characterization of Au/Gd bimetallic nanostructure as potential contrast agents in CT and MR imaging

Rashed Ahmadyani¹, Hamed Ahmadyani¹, Milad Moradi², Sajad Moradi², Mohsen Shahlaei², Saleh Salehi Zahabi³, Faranak Aghaz², Kave Moloudi³, Negin Farhadian^{2*}

¹Students Research Committee, School of Medicine, Kermanshah University of Medical Sciences, Kermanshah, Iran

²Nano Drug Delivery Research Center, Health Technology Institute, Kermanshah University of Medical Sciences, Kermanshah, Iran

³Department of Radiology and Nuclear Medicine, Alley School of Medicine, Kermanshah University of Medical Sciences, Kermanshah, Iran

Article Info



Article Type:

Original Article

Article History:

Received: 15 Apr. 2024

Revised: 19 May 2024

Accepted: 28 May 2024

ePublished: 3 Aug. 2024

Keywords:

Bimetal nanostructure
 Contrast agents
 CT imaging
 MR imaging

Abstract

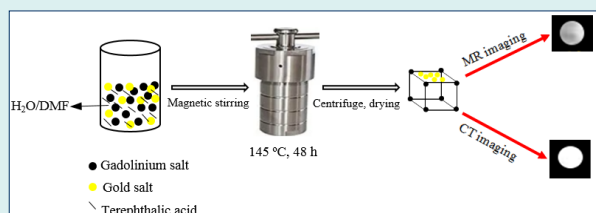
Introduction: Multimodal contrast agents play an important role in early diagnosis of diseases and monitoring the treatment outcomes by increasing the accuracy and clarity of images.

Methods: Herein, a one-step simple hydrothermal route is utilized to prepare the

gadolinium-1,4 H₂BDC- metal-organic framework (Gd-BDC-MOF) nanoparticles decorated with gold nanoclusters. The physicochemical properties of bimetal nanostructures were evaluated, their safety and ability to enhance contrast in both CT and MR imaging were also examined.

Results: The spherical nano-sized Au decorated Gd bimetal nanostructures have an average diameter of 64 nm. The presence of both Au and Gd metals in the prepared nanostructure was confirmed using EDAX. The XRD pattern shows that, in the hydrothermal synthesis of two metals using a terephthalic acid linker, gold nanoclusters are decorated onto the gadolinium metal organic framework. The FTIR analysis confirmed the attachment of Gd to the carboxylate group of the organic linker. The bimetal nanostructure sample with a concentration of 40 mM showed similar X-ray attenuation to that of iodine at a concentration of 128 mM. At a magnetic field strength of 1.5 T, the longitudinal relaxivity value of the bimetal nanostructure was determined to be 13.635 mM⁻¹s⁻¹. The MTT assay demonstrated the cytocompatibility and safety of the contrast agent synthesized for biomedical applications.

Conclusion: The fabricated bimetal nanostructure exhibits dose-dependent positive contrast enhancement in both MR and CT imaging techniques, making it a promising candidate for use as a contrast agent in medical applications.



Introduction

From the economic and practical point of view, it is necessary to develop new contrast agents that maximize the diagnostic potential of current imaging tools. Multifunctional contrast-enhanced nanomaterials overcome the limitations of single contrast agents and enable multimodal imaging for biological, molecular, diagnostic and therapeutic applications.¹ Multifunctional nanomaterials have shown considerable applications in various fields of biomedicine, including drug/gene delivery, disease diagnosis, and treatment monitoring.¹⁻⁴

In this case, gold nanoparticles (AuNPs) of specific shapes and sizes can be utilized for both imaging and photothermal therapy purposes. Researchers have explored the potential of utilizing exogenous nanostructures, including metals such as Au, Ag, and Pt,^{5,6} as well as quantum dots,^{7,8} iron and lanthanide oxides⁹⁻¹² for various bioimaging applications. Current imaging modalities, including optical imaging, ultrasound (US), computed tomography (CT), positron emission tomography (PET), magnetic resonance imaging (MRI), and single photon emission computed tomography (SPECT), each possess distinct



*Corresponding author: Negin Farhadian, Email: neginfarhadian@yahoo.com



© 2025 The Author(s). This work is published by BioImpacts as an open access article distributed under the terms of the Creative Commons Attribution Non-Commercial License (<http://creativecommons.org/licenses/by-nc/4.0/>). Non-commercial uses of the work are permitted, provided the original work is properly cited.

advantages and disadvantages.¹³ Given the inherent constraints of each imaging technique, it is improbable to provide a complete diagnostic assessment using a single approach. Therefore, multimodal imaging technologies have been developed to integrate the advantages of different imaging techniques into a single system. Combined methods include PET/CT, MRI/PET, CT/SPECT, and MRI/optical imaging.¹⁴⁻¹⁸ CT is a clinically available and cost-effective imaging technology that provides 3D tomographic information with high spatial resolution. However, it suffers from limited soft-tissue resolution due to restricted density differences.¹⁹ MRI, on the other hand, is a non-invasive and powerful imaging technology that offers high-resolution visualization of soft tissues with no ionizing radiation and unlimited tissue penetration depth.²⁰⁻²³ However, one drawback of this technique is its low sensitivity.²⁴ The simultaneous use of CT and MRI techniques can alleviate the limitations of each individual modality and facilitate precise diagnosis through improving image sensitivity and contrast.²⁵ To achieve this goal, the development of a single multimodal nanostructure through the integration of various contrast agents can enable effective resolution simultaneously in both CT and MRI techniques.²⁶ Furthermore, utilizing a single contrast agent for multiple imaging modalities not only reduces treatment costs but also enhances patient comfort and health. Gadolinium (Gd) chelates are extensively used in clinical MR imaging as they effectively shorten the longitudinal relaxation time (T1) of water protons.²⁷ Gold nanostructures have garnered significant attention as potential contrast agents for CT due to their good biocompatibility, high atomic number, tunable morphology, and high X-ray attenuation coefficient.²⁸ Although some studies²⁹⁻³² have reported the combination of Au nanoclusters with Gd chelates for multimodal MR/CT imaging, their synthesis faces challenges in terms of further functionalization of small-sized Gd chelates. Additionally, the process requires two different steps and involves a complicated chemical conjugation process. Therefore, it is necessary to develop alternative synthetic methodologies for bimetal nanostructure preparation that can provide effective contrast in both CT and MRI methodologies. To the best of our knowledge, the hydrothermal synthesis of a bimetal nanostructure containing Gd and Au metals in a one-pot simple route using terephthalic acid as an organic linker has not been performed. The potential of the prepared bimetal nanostructure was examined for both X-ray attenuation in CT and as a positive contrast agent in MRI.

Material and Methods

Chemical reagents

Gadolinium (III) nitrate hexahydrate, chloroauric acid, terephthalic acid (98%), and N,N-dimethylformamide (DMF) were purchased from Sigma-Aldrich. Iodixanol

(VISODIX 320 mg/ml, 50 ml) was purchased from Daroupakhsh Distribution Co, Iran. Also, 3-(4,5-Dimethylthiazol-2-yl)-2,5-diphenyltetrazolium bromide (MTT reagent), phosphate-buffered saline (PBS), fetal bovine serum (FBS), and Dulbecco's modified eagle medium/nutrient mixture F-12 (DMEM/F-12) medium, were obtained from Sigma-Aldrich. The fibroblast cell line was obtained from the Pasteur Institute of Iran (IPI).

Synthesize of bimetal Au decorated Gd MOF nanostructure

The synthesis of nanoparticles is based on the studies that prepared the Gd MOF NPs using hydrothermal route,^{33,34} which has been modified by adding gold. In this regard, a mixture of $Gd(NO_3)_3 \cdot 6H_2O$ (25 mg, 0.055 mmol), $H(AuCl_4) \cdot 3H_2O$ (10 mg, 0.025 mmol), terephthalic acid (12.5 mg, 0.075 mmol), 80 ml DMF and distilled water (1:1) was poured into a Teflon-lined stainless-steel autoclave and heated at 145 °C for 2 days. After cooling the autoclave to ambient temperature, the resulting solution was centrifuged, washed with distilled water, and air-dried to obtain crystalline powder of NPs.

Characterization

The zeta potential, hydrodynamic diameter, and polydispersity index (PDI) data for Au-decorated Gd MOF nanostructures were determined using Zetasizer apparatus (Malvern Instruments Ltd., UK). Transmission electron microscopy (TEM) and scanning electron microscopy images were obtained using a TEM Philips EM 208S and SEM VEGA3, respectively. X-ray diffraction (XRD) analysis was conducted using Inel Equaniox 3000 instrument (France) operating at 30 kV and 20 mA, with Cu K α radiation. The FTIR spectra of the bimetal MOF was acquired using a Shimadzu-IR2000 spectrometer. The Iodine and metal contents (Au and Gd) of iodixanol and the bimetal MOF were determined using inductively coupled plasma atomic emission spectrometry (ICP 5300 DV, Perkin-Elmer).

MRI imaging

The MR images were acquired using a 1.5 T MRI scanner (GE Signa HD, USA). The longitudinal relaxation time (T1)-weighted images were recorded using echo sequence scanning with the following imaging parameters: field-of-view (FOV) of 34, slice thickness of 4 mm, TE of 15 ms, and the repetition time (TR) values of 150, 230, 520, 1000, 1800, and 3000 ms. The bandwidth was set to 31.25 kHz. Various concentrations of nanoparticles were prepared, and 300 μ L of each concentration was poured into a 96-well plate for ELISA. All images were analyzed using ImageJ software with the MRI analysis plugin. The signal intensity of each MR image was recorded by selecting the region of interest, and the changes in signal intensities at various repetition times were applied for the nonlinear

fitting of the curves.

CT imaging

For CT imaging, the prepared bimetal nanostructures were dispersed in water at different Au concentrations, and 300 μ l of suspensions were placed into a 96-well plate. The CT contrast ability of Au-decorated Gd MOF was studied using a Siemens CT scan machine at a low magnification of 80 kVp, current of 30 mAs and slice thickness of 0.6 mm. For each sample, X-ray attenuation values were averaged over a region of interest and reported based on Hounsfield units.

In vitro cytotoxicity assay

The cytotoxicity of the nanoparticles was studied through the MTT assay on fibroblast cells (NCBI code: C 192, HSF-PI 16). The cells were divided into two groups without and with different concentrations of nanoparticles (0-40 mM). Afterward, the control and experimental media were collected and washed with sterile PBS to remove any components of the test composite. Then, 50 μ l of MTT color solution (5 mg/mL PBS) was added to each well and incubated for 4 h at 37 $^{\circ}$ C in a humidified atmosphere of 95% air and 5% CO₂. Subsequently, the colored formazan formed in each well was dissolved in 200 μ l of DMSO. The absorbance was measured at 570 nm utilizing a plate reader spectrophotometer (Lonza BioTek ELx808 Absorbance Plate Read). The cell viability chance was calculated using the following formula:

$$\text{Cell viability (\%)} = \frac{A_{570}(\text{sample})}{A_{570}(\text{control})} \times 100$$

Results and Discussion

Characteristics of the Au decorated Gd MOF nanostructure

The average hydrodynamic diameters of Au-decorated Gd MOF nanostructure was measured to be 64 nm. The particles had a positive charge and a zeta potential of 32.1 mV. They were well-dispersed in water and had a low polydispersion index (PDI) of 0.347, as determined by DLS analysis. Fig. 1 illustrates the microscopic morphology, structure, and chemical composition of the nano-sized Au-decorated Gd bimetal structures, which were investigated using SEM, TEM, and EDAX analysis. It is evident from the SEM image that the majority of the nanoparticles exhibit a relatively spherical shape, and they are uniformly distributed and loosely agglomerated. The TEM images displayed the presence of polyhedral crystals with dimensions of about 50 nm. The energy dispersive X-ray spectra confirmed the bimetallic composition of the synthesized NPs.

The XRD pattern of the as-synthesized nano-sized Au decorated Gd MOF bimetal structure presented in Fig. 2. A series of characteristics diffraction peaks corresponding to both Gd and Au metals indicated the polycrystalline lattice structure of the nanoparticles. The observed diffraction peaks related to Gd were consistent with the reference pattern of Gd-BDC-MOF reported previously.³⁵ Additionally, the slight displacements of the diffraction peak positions from their expected angles were attributed to the interaction between the bimetal centers in the formed nanostructure. The absence of additional peaks in the pattern confirmed the phase purity of the formed

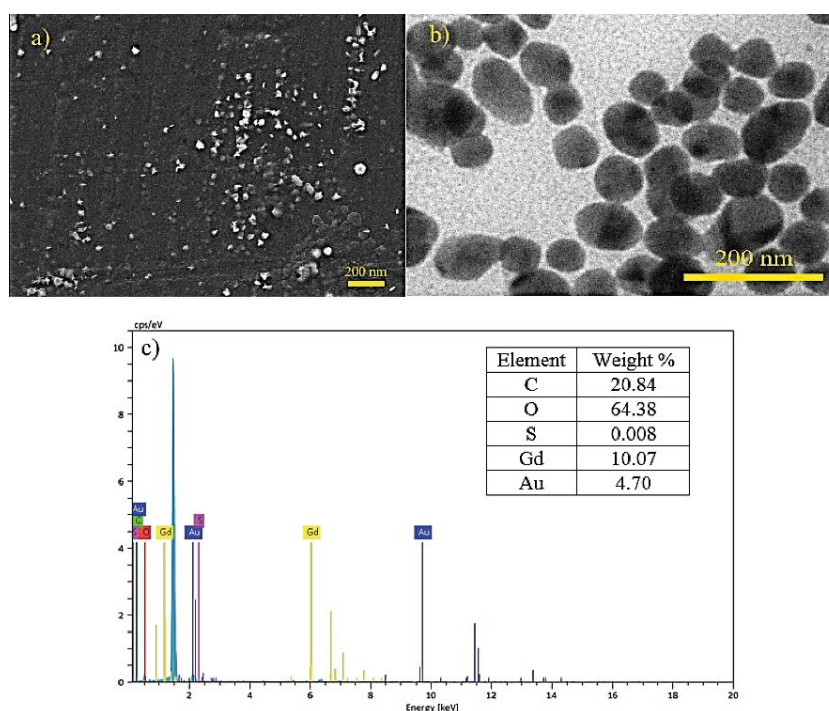


Fig. 1. a) SEM, b) TEM and c) EDAX analysis of the as-synthesized bimetal nanostructure.

crystal.

The FTIR spectrum of Au-decorated Gd MOF bimetal nanostructure is illustrated in Fig. 3. The broad band at 3400 cm^{-1} is attributed to the OH stretching of water molecules. The band at 1647 cm^{-1} corresponds to the C=O stretch of carbonyl group. A band related to the stretching mode of -CH is observed at 2930 cm^{-1} . A band at 1390 cm^{-1} corresponds to the C-C symmetric vibration.³⁶ The C-O stretch appears at 1255 cm^{-1} . Moreover, the two bands at 478 and 663 cm^{-1} are related to the Gd-O stretching vibrations that confirm the binding of Gd to the carboxylate group of the organic linker.³⁷⁻³⁹

In vitro X-ray attenuation measurements

To examine the effectiveness of the Au-decorated Gd MOF nanostructures as a CT contrast agent, different concentration of the bimetal nanostructure in water were prepared, and their contrast values were compared with Iodixanol. The in vitro CT imaging is illustrated in Fig. 4. As illustrated, the bimetal nanostructure exhibited CT contrast capability at all examined concentrations. Increasing the concentration of the bimetal nanostructures and iodine resulted in an increased contrast in the images. According to the similar brightness observed in the image, it can be concluded that a concentration of 40 mM of bimetal nanostructures provides the same contrast as 128 mM of iodine. The values of attenuated CT numbers

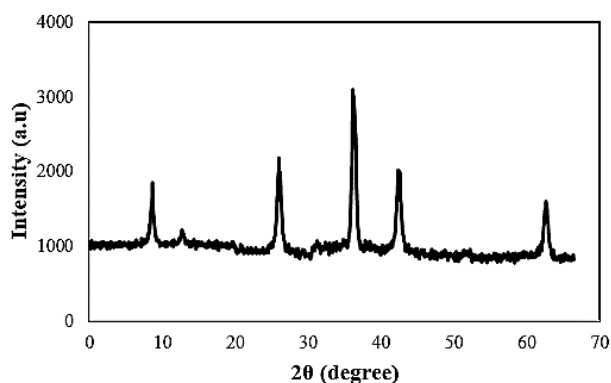


Fig. 2. XRD pattern of the as-synthesized bimetal nanostructure

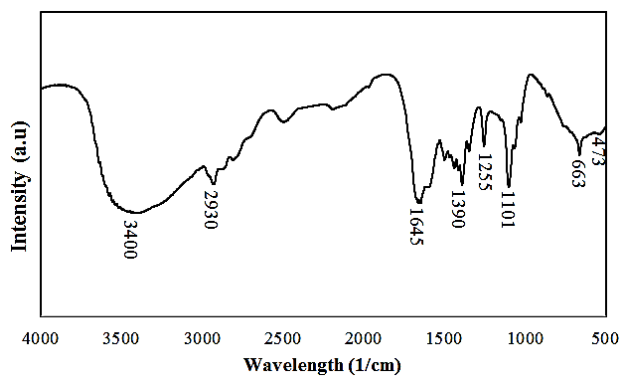


Fig. 3. FTIR spectra of the as-synthesized bimetal nanostructure

for bimetal nanostructures and iodine were measured as 608.2 HU and 612.5 HU , respectively. Compared to iodine, gold has a higher atomic number and electron density, resulting in higher X-ray attenuation. It should also be mentioned that the concentration of bimetal nanostructures, containing both gold and gadolinium elements, is taken into account in CT imaging, because Gd is an element with a high atomic number that can cause a large attenuation coefficient in CT imaging.^{40,41} Finally, the comparable X-ray attenuation of the synthesized nanoparticles to that of clinically used contrast agents confirms the feasibility of the Au-decorated Gd MOF bimetal nanostructure for CT imaging.

In vitro MR imaging

The relaxivity values of the Au-decorated Gd MOF nanostructures were studied at a 1.5 T magnetic field. The MR images of samples with different concentrations of gadolinium ions and the dependence of T1 relaxation time on metal concentration are presented in the Fig. 5. An enhancement in brightness was observed with increasing Gd concentration. A clear linear relationship between the inverse relaxation time and metal concentration was evident. From the slope of $1/T_1$ values versus concentration, the r_1 value of the Au-decorated Gd bimetal nanostructure turned out to be $13.635\text{ mM}^{-1}\text{ s}^{-1}$. These mixed metal nanostructures exhibited higher longitudinal relaxivity compared to

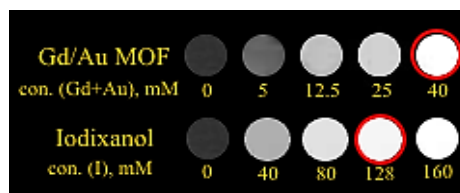


Fig. 4. CT images of different concentrations of the as-synthesized bimetal nanostructure and iodixanol

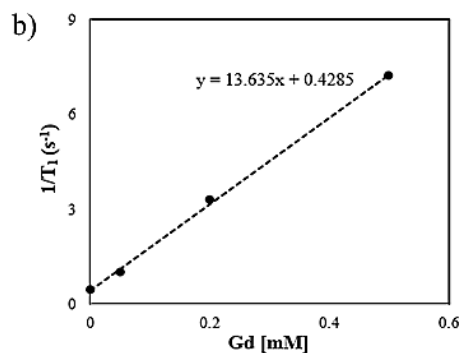


Fig. 5. a) T1 weighted MR images of the as-synthesized bimetal nanostructure, and b) relaxation rate versus different concentration of Gd

the clinically used contrast agent Magnevist complex ($3.58 \text{ mM}^{-1}\text{s}^{-1}$).⁴² The integrated bimetal contrast agent of Gd MOF with decorated Au nanoclusters, instead of combining modified Gd chelates with gold nanoparticles, has a larger size and a high payload of magnetic centers (Gd^{3+}), resulting in an enhanced retention time and relaxation rates.⁴³ The positive MRI signal enhancement showed by these bimetal nanostructures, compared to water, demonstrated their ability as an efficient MRI contrast agent.

In vitro cytotoxicity

MTT assay was used to investigate the cytotoxicity of nano-sized Au-decorated Gd MOF bimetal structure at different concentrations on fibroblast cell lines (Fig. 6). When compared with the control group, the nanostructure did not significantly decrease cell viability percentages in fibroblast cells after 24 and 48 h. This indicates the cytocompatibility and safety of the nanostructure for biomedical applications.

Most of the developed nanoparticles for dual-modal CT/MR biomedical imaging have focused on adding Au NPs to Gd chelates. The disadvantages of these NPs is the low Gd^{3+} magnetic payload per particle and some limitations related to further surface functionalization. The Gd metal organic frameworks can overcome such challenges of those contrast agents prepared using Gd chelates due to their tunable size and high metal loading as well as multivalency.²⁶ Furthermore, the good structural integrity of MOFs leading to reduced free Gd ions concentration in the environment which results in low toxicity related side effects.⁴⁴ Previous studies synthesized Gd MOF NPs using surfactant-assisted microemulsion method and exhibited enhanced T1 relaxation properties.^{45,46} The drawback of such emulsion based method is using the large quantity of harmful organic solvents.⁴⁴ In another work by Tian et al,²⁶ nanoparticles of Gd MOF were prepared by solvothermal method. The MOFs were then connected AuNPs using poly acrylic acid as a bridge. These hybrid NPs showed CT and MRI contrast enhancement. A range of longitudinal relaxivity values were obtained in the vast majority of works previously conducted on multimodal

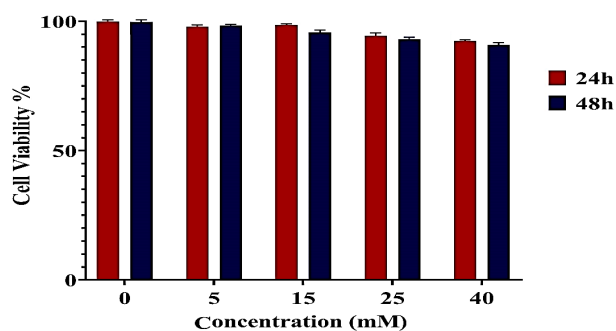


Fig. 6. In-vitro cytotoxicity of the bimetal nanostructure on fibroblast cells compared to control (concentration = 0).

contrast materials containing both Gd and Au metals. These variations are attributed to the particle morphology and the magnetic field strength which affect the MRI relaxivities.⁴⁷ However, the concentration of Au NPs is an influential parameter for CT contrast than their size and shape.⁴⁸ Similarly, the synthesized bimetal NPs in the present study are also able to increase the contrast of the images in both CT and MRI methods. The advantage of this study is the one-step synthesis of Au/Gd complex with a simple, low-cost and environmentally friendly route, in which the least amount of hazardous chemicals is utilized.

Conclusion

The one-pot hydrothermal synthesis route is a useful method for the successful preparation of a bimetal Au-decorated Gd MOF nanostructure, which can be used as a positive contrast agent in both CT and MRI modalities. The structure of the Au-decorated Gd-BDC-MOF was established through XRD analysis. The 40 mM bimetal contrast agent has an attenuation of 608 HU in the CT experiment. The Gd-BDC-MOF nanostructure, which is larger in size and has a higher paramagnetic Gd payload, exhibited a higher longitudinal relaxivity compared to that of the clinically used contrast agent Magnevist complex. The signal enhancement by the proposed bimetal nanostructure compared to water in both CT and MRI techniques highlights its potential as an efficient bimodal contrast agent.

Acknowledgments

The authors are acknowledged to the Kermanshah University of Medical Sciences for supporting the work (grant no: 990670).

Authors' Contribution

Conceptualization: Negin Farhadian, Sajad Moradi, Mohsen Shahlaei.

Data curation: Negin Farhadian, Sajad Moradi, Milad Moradi, Mohsen Shahlaei.

Formal analysis: Negin Farhadian, Saleh Salehi Zahabi, Farnak Aghaz, Kave Moloudi.

Funding acquisition: Negin Farhadian.

Investigation: Negin Farhadian, Rashed Ahmadyani, Hamed Ahmadyani, Sajad Moradi, Milad Moradi, Saleh Salehi Zahabi, Farnak Aghaz, Kave Moloudi.

Methodology: Negin Farhadian, Rashed Ahmadyani, Hamed Ahmadyani, Saleh Salehi Zahabi, Farnak Aghaz, Kave Moloudi.

Project administration: Negin Farhadian, Sajad Moradi, Mohsen Shahlaei.

Resources: Negin Farhadian, Rashed Ahmadyani, Hamed Ahmadyani.

Software: Negin Farhadian.

Supervision: Negin Farhadian, Sajad Moradi, Mohsen Shahlaei.

Validation: Negin Farhadian, Sajad Moradi, Mohsen Shahlaei, Milad Moradi.

Visualization: Negin Farhadian, Saleh Salehi Zahabi, Farnak Aghaz, Kave Moloudi.

Writing—original draft: Negin Farhadian, Rashed Ahmadyani, Hamed Ahmadyani, Saleh Salehi Zahabi, Farnak Aghaz, Kave Moloudi.

Writing—review & editing: Sajad Moradi, Mohsen Shahlaei, Milad Moradi.

Competing Interests

All authors have no conflict of interest to declare.

Research Highlights

- Recently, multimodal contrast agents developed for biomedical imaging can provide comprehensive diagnostic information, reduce costs and improve patient care.
- This work introduces a new complex of Au-decorated Gd MOF nanostructure synthesized in a simple and one-pot hydrothermal route for MRI/CT.

Ethical Statement

Ethics Committee of Kermanshah University of Medical Sciences was confirmed this study (IR.KUMS.REC.1399.228).

Funding

Kermanshah University of Medical Sciences (grant no: 990670).

References

- Jin Y, Jia C, Huang SW, O'Donnell M, Gao X. Multifunctional nanoparticles as coupled contrast agents. *Nat Commun* **2010**; 1: 41. doi: 10.1038/ncomms1042.
- Cheng L, Yang K, Li Y, Zeng X, Shao M, Lee ST, et al. Multifunctional nanoparticles for upconversion luminescence/MR multimodal imaging and magnetically targeted photothermal therapy. *Biomaterials* **2012**; 33: 2215-22. doi: 10.1016/j.biomaterials.2011.11.069.
- Melancon MP, Zhou M, Li C. Cancer theranostics with near-infrared light-activatable multimodal nanoparticles. *Acc Chem Res* **2011**; 44: 947-56. doi: 10.1021/ar200022e.
- Park K, Lee S, Kang E, Kim K, Choi K, Kwon IC. New generation of multifunctional nanoparticles for cancer imaging and therapy. *Adv Funct Mater* **2009**; 19: 1553-66. doi: 10.1002/adfm.200801655.
- Lok CN, Zou T, Zhang JJ, Lin IW, Che CM. Controlled-release systems for metal-based nanomedicine: encapsulated/self-assembled nanoparticles of anticancer gold(III)/platinum(II) complexes and antimicrobial silver nanoparticles. *Adv Mater* **2014**; 26: 5550-7. doi: 10.1002/adma.201305617.
- Shafikov MZ, Suleymanova AF, Kutta RJ, Gorski A, Kowalczyk A, Gapińska M, et al. Ligand design and nuclearity variation towards dual emissive Pt(ii) complexes for singlet oxygen generation, dual channel bioimaging, and theranostics. *J Mater Chem C* **2022**; 10: 5636-47. doi: 10.1039/d2tc00257d.
- Martynenko IV, Litvin AP, Purcell-Milton F, Baranov AV, Fedorov AV, Gun'ko YK. Application of semiconductor quantum dots in bioimaging and biosensing. *J Mater Chem B* **2017**; 5: 6701-27. doi: 10.1039/c7tb01425b.
- Li Z, Wang Q, Zhou Z, Zhao S, Zhong S, Xu L, et al. Green synthesis of carbon quantum dots from corn stalk shell by hydrothermal approach in near-critical water and applications in detecting and bioimaging. *Microchem J* **2021**; 166: 106250. doi: 10.1016/j.microc.2021.106250.
- Comby S, Surender EM, Kotova O, Truman LK, Molloy JK, Gunnlaugsson T. Lanthanide-functionalized nanoparticles as MRI and luminescent probes for sensing and/or imaging applications. *Inorg Chem* **2014**; 53: 1867-79. doi: 10.1021/ic4023568.
- Liu F, Laurent S, Fattahi H, Vander Elst L, Muller RN. Superparamagnetic nanosystems based on iron oxide nanoparticles for biomedical imaging. *Nanomedicine (Lond)* **2011**; 6: 519-28. doi: 10.2217/nnm.11.16.
- Chávez-García D, Sengar P, Juárez-Moreno K, Flores DL, Calderón I, Barrera J, et al. Luminescence properties and cell uptake analysis of Y2O3:Eu, Bi nanophosphors for bio-imaging applications. *J Mater Res Technol* **2021**; 10: 797-807. doi: 10.1016/j.jmrt.2020.11.071.
- Papadopoulou S, Kolokithas-Ntoukas A, Salvanou EA, Gaitanis A, Xanthopoulos S, Avgoustakis K, et al. Chelator-free/chelator-mediated radiolabeling of colloidal stabilized iron oxide nanoparticles for biomedical imaging. *Nanomaterials (Basel)* **2021**; 11: 1677. doi: 10.3390/nano11071677.
- Lee DE, Koo H, Sun IC, Ryu JH, Kim K, Kwon IC. Multifunctional nanoparticles for multimodal imaging and theragnosis. *Chem Soc Rev* **2012**; 41: 2656-72. doi: 10.1039/c2cs15261d.
- Englmeier KH, Seemann MD. Multimodal virtual bronchoscopy using PET/CT images. *Comput Aided Surg* **2008**; 13: 106-13. doi: 10.3109/10929080801954164.
- Larson TA, Bankson J, Aaron J, Sokolov K. Hybrid plasmonic magnetic nanoparticles as molecular specific agents for MRI/optical imaging and photothermal therapy of cancer cells. *Nanotechnology* **2007**; 18: 325101. doi: 10.1088/0957-4484/18/32/325101.
- Hansen JA, Naghavi-Behzad M, Gerke O, Baun C, Falch K, Duvnjak S, et al. Diagnosis of bone metastases in breast cancer: lesion-based sensitivity of dual-time-point FDG-PET/CT compared to low-dose CT and bone scintigraphy. *PLoS One* **2021**; 16: e0260066. doi: 10.1371/journal.pone.0260066.
- Panigrahy C, Seal A, Gonzalo-Martín C, Pathak P, Jalal AS. Parameter adaptive unit-linking pulse coupled neural network-based MRI-PET/SPECT image fusion. *Biomed Signal Process Control* **2023**; 83: 104659. doi: 10.1016/j.bspc.2023.104659.
- Ritt P, Kuwert T. Quantitative SPECT/CT—technique and clinical applications. In: Schober O, Kiessling F, Debus J, eds. *Molecular Imaging in Oncology*. Cham: Springer; **2020**. p. 565-90. doi: 10.1007/978-3-030-42618-7_17.
- Zhou B, Zheng L, Peng C, Li D, Li J, Wen S, et al. Synthesis and characterization of PEGylated polyethylenimine-entrapped gold nanoparticles for blood pool and tumor CT imaging. *ACS Appl Mater Interfaces* **2014**; 6: 17190-9. doi: 10.1021/am505006z.
- Cai Y, Wang Y, Zhang T, Pan Y. Gadolinium-labeled ferritin nanoparticles as T1 contrast agents for magnetic resonance imaging of tumors. *ACS Appl Nano Mater* **2020**; 3: 8771-83. doi: 10.1021/acsnm.0c01563.
- Caspani S, Magalhães R, Araújo JP, Sousa CT. Magnetic nanomaterials as contrast agents for MRI. *Materials (Basel)* **2020**; 13: 2586. doi: 10.3390/ma13112586.
- Chen C, Ge J, Gao Y, Chen L, Cui J, Zeng J, et al. Ultrasmall superparamagnetic iron oxide nanoparticles: a next generation contrast agent for magnetic resonance imaging. *Wiley Interdiscip Rev Nanomed Nanobiotechnol* **2022**; 14: e1740. doi: 10.1002/wnan.1740.
- Kim KS, Park W, Hu J, Bae YH, Na K. A cancer-recognizable MRI contrast agents using pH-responsive polymeric micelle. *Biomaterials* **2014**; 35: 337-43. doi: 10.1016/j.biomaterials.2013.10.004.
- Mahmoudi M, Serpooshan V, Laurent S. Engineered nanoparticles for biomolecular imaging. *Nanoscale* **2011**; 3: 3007-26. doi: 10.1039/c1nr10326a.
- Yue L, Wang J, Dai Z, Hu Z, Chen X, Qi Y, et al. pH-responsive, self-sacrificial nanotheranostic agent for potential in vivo and in vitro dual modal MRI/CT imaging, real-time, and in situ monitoring of cancer therapy. *Bioconjug Chem* **2017**; 28: 400-9. doi: 10.1021/acs.bioconjchem.6b00562.
- Tian C, Zhu L, Lin F, Boyes SG. Poly(acrylic acid) bridged gadolinium metal-organic framework-gold nanoparticle composites as contrast agents for computed tomography and magnetic resonance bimodal imaging. *ACS Appl Mater Interfaces* **2015**; 7: 17765-75. doi: 10.1021/acsami.5b03998.
- Xu Q, Zhu L, Yu M, Feng F, An L, Xing C, et al. Gadolinium(III) chelated conjugated polymer as a potential MRI contrast agent. *Polymer* **2010**; 51: 1336-40. doi: 10.1016/j.polymer.2009.04.003.
- Dreaden EC, Alkilany AM, Huang X, Murphy CJ, El-Sayed MA. The golden age: gold nanoparticles for biomedicine. *Chem Soc Rev* **2012**; 41: 2740-79. doi: 10.1039/c1cs15237h.
- Alric C, Taleb J, Le Duc G, Mandon C, Billotey C, Le Meur-Herland A, et al. Gadolinium chelate coated gold nanoparticles as contrast agents for both X-ray computed tomography and

- magnetic resonance imaging. *J Am Chem Soc* **2008**; 130: 5908-15. doi: 10.1021/ja078176p.
30. Kim HK, Jung HY, Park JA, Huh MI, Jung JC, Chang Y, et al. Gold nanoparticles coated with gadolinium-DTPA-bisamide conjugate of penicillamine (Au@GdL) as a T1-weighted blood pool contrast agent. *J Mater Chem* **2010**; 20: 5411-7. doi: 10.1039/c0jm00163e.
31. Park JA, Reddy PA, Kim HK, Kim IS, Kim GC, Chang Y, et al. Gold nanoparticles functionalised by Gd-complex of DTPA-bis(amide) conjugate of glutathione as an MRI contrast agent. *Bioorg Med Chem Lett* **2008**; 18: 6135-7. doi: 10.1016/j.bmcl.2008.10.017.
32. Nasiruzzaman SM, Kim HK, Park J, Chang Y, Kim TJ. Gold nanoparticles coated with Gd-chelate as a potential CT/MRI bimodal contrast agent. *Bull Korean Chem Soc* **2010**; 31: 1177-81. doi: 10.5012/bkcs.2010.31.5.1177.
33. Ghosh P, Maity T, Biswas S, Debnath R, Koner S. Thermally stable and robust gadolinium-based metal-organic framework: synthesis, structure and heterogeneous catalytic O-arylation reaction. *Polyhedron* **2021**; 194: 114934. doi: 10.1016/j.poly.2020.114934.
34. Wei D, Xin Y, Rong Y, Li Y, Zhang C, Chen Q, et al. A mesoporous Gd-MOF with Lewis basic sites for 5-Fu delivery and inhibition of human lung cancer cells in vivo and in vitro. *J Inorg Organomet Polym Mater* **2020**; 30: 1121-31. doi: 10.1007/s10904-019-01305-x.
35. Icten O. Preparation of gadolinium-based metal-organic frameworks and the modification with boron-10 isotope: a potential dual agent for MRI and neutron capture therapy applications. *ChemistrySelect* **2021**; 6: 1900-10. doi: 10.1002/slct.202100438.
36. Ji Y, Yang X, Ji Z, Zhu L, Ma N, Chen D, et al. DFT-calculated IR spectrum amide I, II, and III band contributions of N-methylacetamide fine components. *ACS Omega* **2020**; 5: 8572-8. doi: 10.1021/acsomega.9b04421.
37. Li G, Peng C, Li C, Yang P, Hou Z, Fan Y, et al. Shape-controllable synthesis and morphology-dependent luminescence properties of GaOOH:Dy³⁺ and beta-Ga₂O₃:Dy³⁺. *Inorg Chem* **2010**; 49: 1449-57. doi: 10.1021/ic901682x.
38. Taş AC, Majewski PJ, Aldinger F. Synthesis of gallium oxide hydroxide crystals in aqueous solutions with or without urea and their calcination behavior. *J Am Ceram Soc* **2002**; 85: 1421-9. doi: 10.1111/j.1151-2916.2002.tb00291.x.
39. Zhao Y, Frost RL, Yang J, Martens WN. Size and morphology control of gallium oxide hydroxide GaOOH, nano- to micro-sized particles by soft-chemistry route without surfactant. *J Phys Chem C* **2008**; 112: 3568-79. doi: 10.1021/jp710545p.
40. Liu Y, Ai K, Lu L. Nanoparticulate X-ray computed tomography contrast agents: from design validation to in vivo applications. *Acc Chem Res* **2012**; 45: 1817-27. doi: 10.1021/ar300150c.
41. Lusic H, Grinstaff MW. X-ray-computed tomography contrast agents. *Chem Rev* **2013**; 113: 1641-66. doi: 10.1021/cr200358s.
42. Xia A, Chen M, Gao Y, Wu D, Feng W, Li F. Gd³⁺ complex-modified NaLuF₄-based upconversion nanophosphors for trimodality imaging of NIR-to-NIR upconversion luminescence, X-ray computed tomography and magnetic resonance. *Biomaterials* **2012**; 33: 5394-405. doi: 10.1016/j.biomaterials.2012.04.025.
43. Lin W, Hyeon T, Lanza GM, Zhang M, Meade TJ. Magnetic nanoparticles for early detection of cancer by magnetic resonance imaging. *MRS Bull* **2009**; 34: 441-8. doi: 10.1557/mrs2009.120.
44. Kundu T, Mitra S, Patra P, Goswami A, Díaz Díaz D, Banerjee R. Mechanical downsizing of a gadolinium(III)-based metal-organic framework for anticancer drug delivery. *Chemistry* **2014**; 20: 10514-8. doi: 10.1002/chem.201402244.
45. Rieter WJ, Taylor KM, An H, Lin W, Lin W. Nanoscale metal-organic frameworks as potential multimodal contrast enhancing agents. *J Am Chem Soc* **2006**; 128: 9024-5. doi: 10.1021/ja0627444.
46. Taylor KM, Jin A, Lin W. Surfactant-assisted synthesis of nanoscale gadolinium metal-organic frameworks for potential multimodal imaging. *Angew Chem Int Ed Engl* **2008**; 47: 7722-5. doi: 10.1002/anie.200802911.
47. Hatakeyama W, Sanchez TJ, Rowe MD, Serkova NJ, Liberatore MW, Boyes SG. Synthesis of gadolinium nanoscale metal-organic framework with hydrotropes: manipulation of particle size and magnetic resonance imaging capability. *ACS Appl Mater Interfaces* **2011**; 3: 1502-10. doi: 10.1021/am200075q.
48. Lee N, Choi SH, Hyeon T. Nano-sized CT contrast agents. *Adv Mater* **2013**; 25: 2641-60. doi: 10.1002/adma.201300081.